DOI: 10.31401/WS.2020.proc.10

Substorm Activity During the Geomagnetic Storm on 25 August 2018

Guineva V., Werner R.

Space Research and Technology Institute BAS, Stara Zagora Department, Bulgaria
E-mail: v_guineva@yahoo.com

Abstract.

The substorms originated during the geomagnetic storm on 25 August 2018 have been studied. This storm developed unexpectedly at the very end of the 24 solar cycle. It was associated with a CME, related to a filament eruption on 20 august 2018. A magnetic cloud (MC) reached the Earth, followed by a corotating interaction region (CIR) in the solar wind. The Bz component of the interplanetary magnetic field (IMF) fold sharp and stayed negative for about 18 hours. This storm appears to be the third by minimal SYM/H value after the storms on 15 March and 22 June 2015. SYM/H reached -206 nT in 7:11 UT on 26 August 2019. The storm was a strong one, $K_{pmax}=7^{+}$ in 6-9 UT on 26 August 2018.

Several substorms were observed during the main and recovery phase of the storm. The occurrence and spreading of the magnetic substorms were studied by IMAGE and INTERMAGNET networks data. For the solar wind and Interplanetary Magnetic Field parameters data from the OMNI data base have been used. SML index was taken from the SuperMag database, and the K_p index – from the Kioto Center for geomagnetism website. The substorms development was examined. The substorms latitudinal extent in the range 92°-108° CGMlon was studied. The magnetic substorms were observed also at middle latitudes as positive magnetic bays. The peculiarities of the substorms and their display at mid-latitudes have been analysed.

Introduction

Substorms are a typical event at auroral latitudes. It is well known that during the substorm expansion phase, the westward electrojet moves fast poleward, usually by consecutive jumps, and under highly enhanced magnetic activity could reach latitudes well above the typical location of the night side auroral oval [e.g., *Akasofu S.-I.*, 1964; *Kisabeth J.L. et al.*, 1974; *Wang H. et al.*, 2005; *Despirak I.V. et al.*, 2008; *Tanskanen E.I. et al.*, 2009, *Clausen et al.*, 2013; *Despirak I. V. et al.*, 2014]. It should be noted also that under disturbed conditions, at increased magnitude of the IMF negative B_Z component, the equatorward boundary of the oval shifts down to about 50° geomagnetic latitude, while its poleward boundary extends to higher latitudes than the usual ones, i.e. the so called “expanded oval” is formed [e.g. *Feldstein Y.L. et al.*, 1967]. It was found out, that the most intensive substorms occur on expanded auroral oval [*Clausen L.B.N. et al.*, 2013]. It is well known also, that in such conditions substorms can be observed at middle and even low latitudes as positive magnetic bays [e.g., *McPherron et al.*, 1973]. *Akasofu et al.*, (1965) explained the positive bays as a result of the low-latitude return currents from the westward electrojet. Later *Akasofu and Meng* (1969) and *Meng and Akasofu* (1969) explained the positive bays as a result of the field aligned currents. *McPherron R.L. et al.*, (1973) developed further the concept of the current system, responsible for the substorm onset and expansion - the Substorm Current Wedge (SCW). By the up-to-date views, the positive bays at mid-latitudes are observed in the substorm expansion phase and are caused by the SCW [*McPherron R.L. et al.*, 2017, 2018].

The aim of this paper is to study the magnetic substorms development under highly disturbed interplanetary and geomagnetic conditions, during the strong magnetic storm on 25 August 2018, and analyze their appearance at middle latitudes.

Data used

The data sources used for the study of magnetic substorms are listed in detail in *Guineva et al*, (2019).

We used the magnetic data from the IMAGE and INTERMAGNET networks. From the IMAGE set, we considered data from the meridional chain stations Polesie (PPN) - Ny Ålesund (NAL), situated in the longitudinal range 98°-112°CGMLon, and covering the latitudinal range from 47º to 75º CGM lat. The chosen INTERMAGNET stations are in the longitudinal range of 92°-104° CGMLon, from 35° to 64° CGMLat. The westward electrojet development was estimated by the time evolution of the equivalent ionospheric currents, computed by the Finish Meteorological Institute (FMI) on-line tool for 22.06° lon. (~112° CGMLon).

The solar wind and Interplanetary Magnetic Field parameters data were taken from the OMNI data base, and the data for the structures in the solar wind - from the catalog of large-scale solar wind phenomena [*Yermolaev, Yu.I. et al.,* 2009]. The SML index was provided from the SuperMag database, and the K_p index – from the Kioto Center for geomagnetism website.

Interplanetary and geomagnetic conditions on 25-29 August 2018

Fig.1 illustrates the interplanetary and geomagnetic conditions in the time period 25-29 August 2018. From up to down the following quantities are displayed: the magnitude of the interplanetary magnetic field (IMF) B_T, the IMF B_Z, the flow velocity V, the flow velocity X-component V_X, the plasma density, temperature (T), pressure (P), and the SML, SYM/H and K_P geomagnetic indices. A filament eruption was registered on the Sun on 20 August 2018, and a related coronal mass ejection (CME) propagated towards the Earth. A magnetic cloud (MC) reached the Earth in 14 UT on 25.08.2018, followed by a high speed stream (HSS). The structures in the solar wind during the examined period are indicated in Fig.1. The Sheath in front of MC initiated a strong storm (k_{pmax}=7^+ in 6-9 UT on 26 August 2018). The initial storm phase began at 6:30 UT, 25.08.2018, and the main phase – from 17:40 UT on 25.08.2018. This storm was the third by minimal SYM/H value after the storms on 15 March and 22 June 2015. SYM/H reached -206 nT in 7:11 UT on 26 August 2019. Ap index was 67.

Magnetic substorms

During the geomagnetic storm, 6 substorms were observed in the examined area (~93°-112° CGMLon, 35°-75° CGMLat) by magnetic data. 3 substorms occurred during the main storm phase, and 3 – during the recovery phase. In all cases, positive magnetic bays were present at middle latitudes. 3 substorms were considered in details: 2 substorms on 25 August 2018, in the beginning of the main storm phase, and one substorm on 27 August 2018, in the late recovery phase. The substorms development is shown in Fig.2 and Fig.3. In Fig. 2, the equivalent ionospheric currents (upper panel) and the X-component of the magnetic field from the IMAGE latitudinal chain PPN-NAL (bottom panel) are given for the substorms on 25 August 2018 (left panels) and 27 August 2018 (right panels). The upper panels demonstrate the westward electrojet dynamics, estimated at the 22.06° geographic longitude (~112° CGMLon). In Fig. 3 the magnetic field X-component at the selected INTERMAGNET stations during the considered substorms (upper panels) and SML indexs, By, Bz, and Vx are presented. The stations CGMLat is indicated to the right. In the figures, the stations are arranged by their magnetic latitude locations. The substorm onsets are indicated by the red vertical lines (determined by PEL, OUJ, OUJ stations data, respectively).

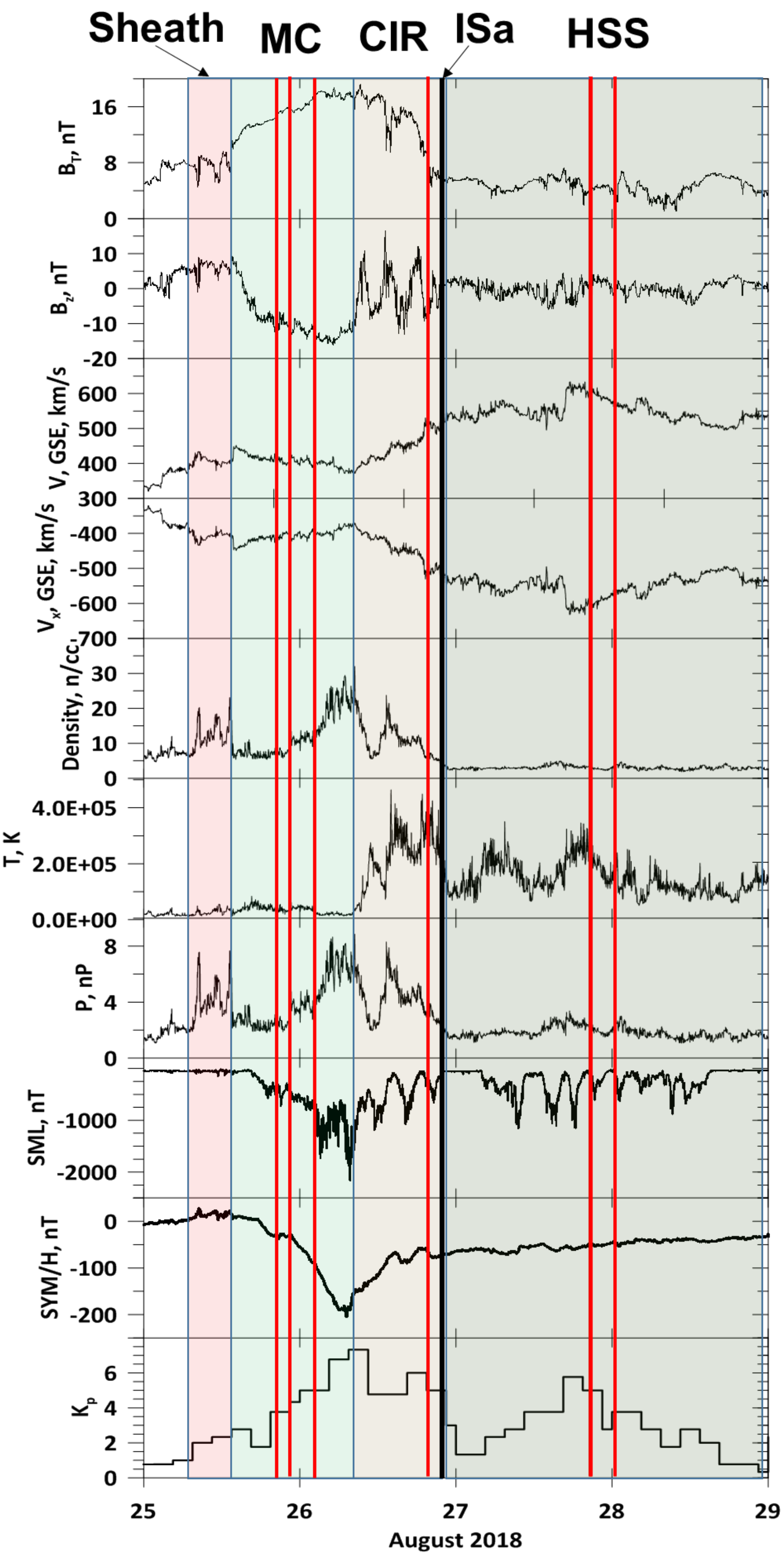

Fig.1. Interplanetary and geomagnetic conditions during the storm on 25 August 2018..The structures in the solar wind are marked by rectangles in different colours and inscribed in the upper part of the figure. The moment of interplanetary shock (IS) arrival is indicated by straight vertical line. The time of the observed substorms are marked by red vertical lines.

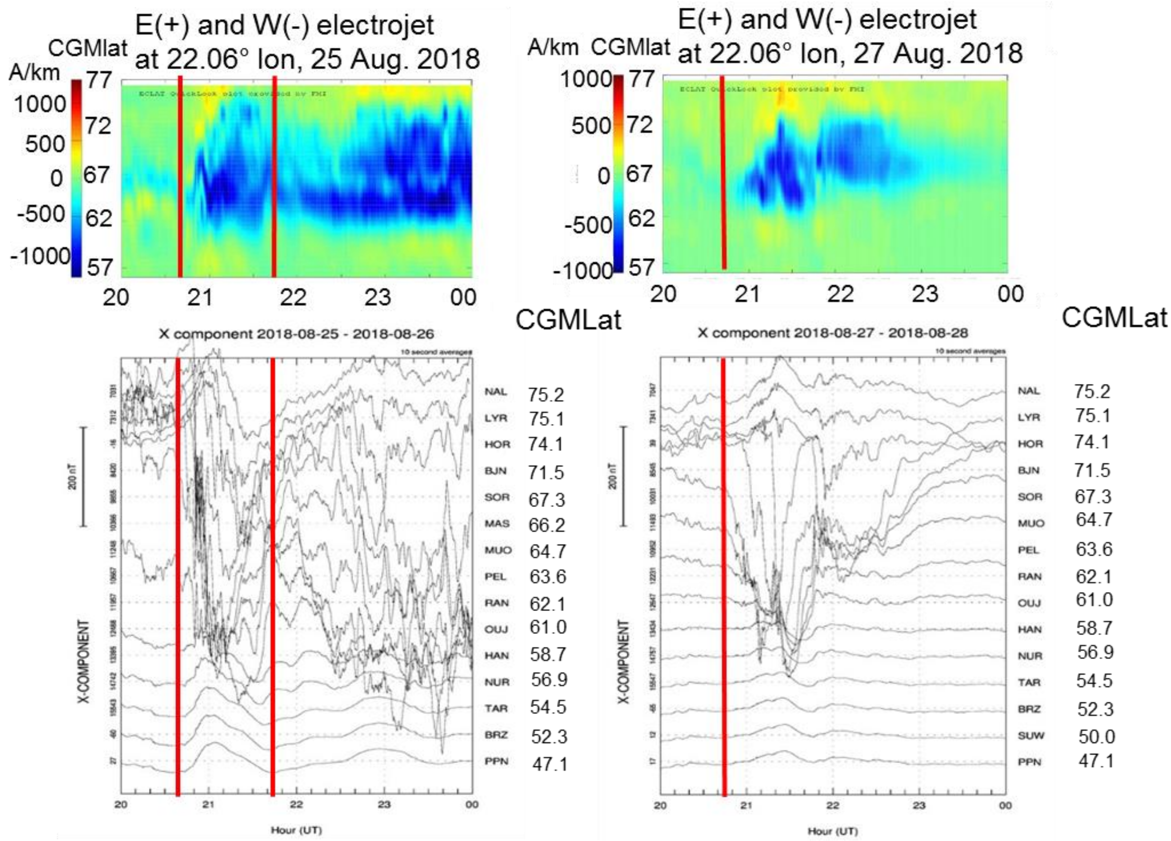

Fig.2. Ionospheric equivalent currents (up), and B_x data from IMAGE latitudinal chain for the substorms (down). The substorms onset times are marked by red vertical lines. The left panels show the substorms on 25 August 2018, during the main storm phase, and the right panels – the substorm on 27 August 2018, in the late recovery phase.

Substorm at 20:40 UT on 25 August 2018

This substorm developed in the beginning of the the main storm phase, at the time of the magnetic cloud (MC) in the solar wind (see Fig. 1). At the substorm onset, SYM/H was -38 nT. The minimal value of SML index during the substorm was -721 nT. The westward electrojet moved fast to the Nord, and surpassed 77° CGMLat. A movement to the South was also observed (Fig.2, left upper panel). The substorm onset was at ~64°-65° CGMLat (PEL-MUO stations). The disturbances in the X-component are clearly expressed to the North, to NAL (75.25° CGMLat) as well as to the South, to OUJ (61.0°CGMlat) (Fig. 2, left bottom panel). At the lower latitudes, a positive bay in the X-component was observed at all stations to the South from HAN (58.7°CGMlat) (Fig. 2, left bottom panel, and Fig. 3, left upper panel). The positive bay lasted about 1 hour.

Substorm at 21:45 UT on 25 August 2018

The second substorm originated just after the first one, also in the beginning of the main phase of the storm, during MC (Fig.1). At the onset, SYM/H was -33 nT. The minimal SML value was -646 nT. The westward electrojet reached 73°-74° to the North and ~61° to the South (Fig.2, left upper panel). The strong disturbances in the X-component begun at 61°-64°CGMLat (OUJ, SOD, LYC stations), reached LYR (75.1° CGMlat) to the North and OUJ (61.0° CGMlat) to the South (Fig. 2, left bottom panel). A positive magnetic bay was registered at NUR (56.9° CGMlat) and at all stations to the South from NUR (Fig. 2, left bottom panel, and Fig. 3, left upper panel). The positive bay lasted about 1 hour 45 min.

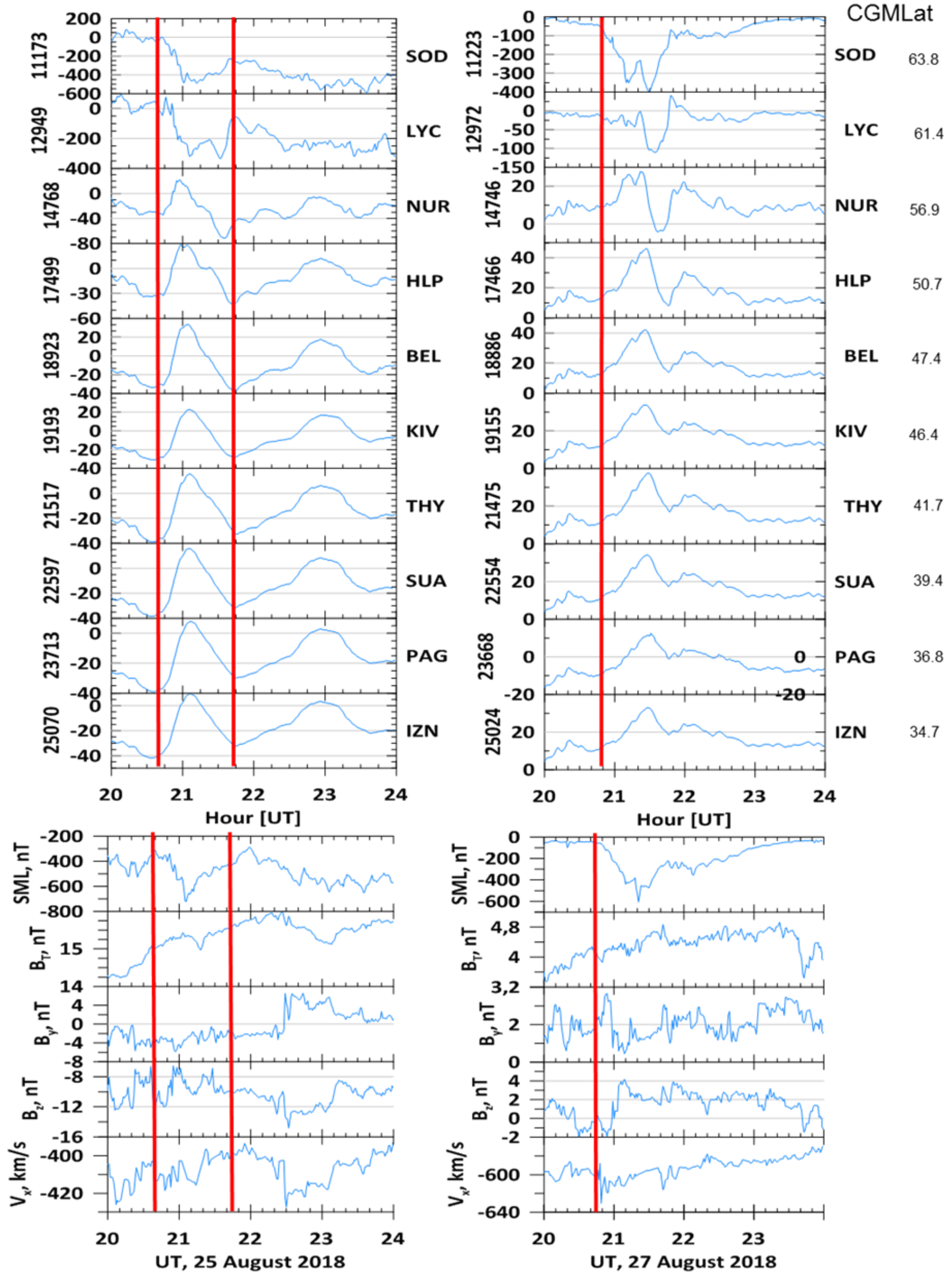

Fig.3. B_x data from INTERMAGNET latitudinal chain for the examined substorms (up), and SML index and some characteristics of the SW and IMF during the same time (down).

Substorm at 20:45 UT on 27 August 2018

The third substorm developed during the late recovery phase of the storm, in the time of a HSS in the solar wind (Fig.1). At the onset, SYM/H was -51 nT. The minimal SML value was -607 nT. The westward electrojet reached 72°-73° to the North and ~63° to the South (Fig.2, right upper panel). The strong disturbances in the X-component begun in the range 62°-67°CGMLat (RAN-SOR stations), reached BJN (71.5° CGMlat) to the North and OUJ (61.0° CGMlat) to the South (Fig. 2, right bottom panel). A positive magnetic bay was registered at NUR (56.9° CGMlat) and at all stations to the South from NUR (Fig. 2, right bottom panel, and Fig. 3, right upper panel). The positive bay lasted about 1 hour.

Conclusions

The magnetic bay sign changed from negative to positive between 59° and 61° CGMlat (between HAN and OUJ stations) during the examined substorms. This boundary is higher than the observed in a previous study: 50°-56° CGMLat [*Guineva et al.*, 2019]. Hence, this boundary depends on the stage of interplanetary and geomagnetic disturbance. The considered in this work cases happened in the beginning of the main phase and in the late recovery phase of the storm, and SYM/H was only several tens nT, while the previously studied events occurred near the maximal storm development or at a shock arrival, or SYM/H was below -150 nT.

References

Akasofu S.-I. (1964). The development of the auroral substorm. Planetary and Space Science, 12(4), 273–282. https://doi.org/10.1016/0032-0633(64)90151-5

Akasofu S.-I., S.Chapman, C.-I. Meng (1965). The polar electrojet. Journal of Atmospheric and Terrestrial Physics, 27(11-12), 1275–1305. https://doi.org/10.1016/0021-9169(65)90087-5

Akasofu, S.-I., & Meng, C.I.: 1969, A study of polar magnetic substorms, J. Geophys. Res., 74(1), 293–313. https://doi.org/10.1029/JA074i001p00293

Clausen L. B. N., S.E. Milan, J. B. H. Baker, J. M. Ruohoniemi, K.-H. Glassmeier, J. C. Coxon, B. J. Anderson (2013). On the influence of open magnetic flux on substorm intensity: Ground- and space-based observations. Journal of Geophysical Research. 118, 2958- 2969, doi:10.1002/jgra.50308.

Despirak I. V., A. A. Lyubchich, H. K. Biernat, A.G. Yakhnin (2008). Poleward expansion of the westward electrojet depending on the solar wind and IMF parameters. Geomagnetism and Aeronomy. 48(3), 284–292.

Despirak I. V., A. A. Lyubchich, N. G. Kleimenova (2014). Polar and High Latitude Substorms and Solar Wind Conditions. Geomagnetism and Aeronomy. 54(5), 619-626.

Feldstein Y. L., G.V. Starkov (1967). Dynamics of auroral belt and geomagnetic disturbances. Planetary and Space Science. 15(2), 209–229.

Guineva V.H., Despirak I.V., Kleimenova N.G. (2019). Substorms manifestation at high and mid-latitudes during two large magnetic storms, Aerospace Res. in Bulgaria, 31, 27-39, https://doi.org/10.3897/arb.v31.e03, http://journal.space.bas.bg/arhiv/n%2031/Articles/3_Guineva.pdf

Kisabeth J. L., G. Rostoker (1974). The expansive phase of magnetospheric substorms: 1. Development of the auroral electrojets and auroral arcs configuration during substorm. Journal of Geophysical Research. 79(7), 972–984.

McPherron R.L., C.T. Russell, M.P. Aubry, (1973). Satellite studies of magnetospheric substorms on August 15, 1968. 9. Phenomenological model for substorms. J. Geophys. Res. 78, 3131

McPherron, R. L., X. Chu (2017). The mid-latitude positive bay and the MPB index of substorm activity. Space Science Reviews, 206(1–4), 91–122. https://doi.org/10.1007/s11214-016-0316-6

McPherron, R. L., X. Chu (2018). The midlatitude positive bay index and the statistics of substorm occurrences. Jurnal of Geophysical Research: Space Physics, 123, 2831-2850. https://doi.org/10.1002/2017JA024766

Meng, C.I., Akasofu, S.-I.: 1969, A study of polar magnetic substorms .2. 3-dimensional current system, J. Geophys. Res., 74(16), 4035–4053. https://doi.org/10.1029/JA074i016p04035

Tanskanen E. I., T. I. Pulkkinen, A. Viljanen, K. Mursula, N. Partamies, J. A. Slavin (2011). From space weather toward space climate time scales: Substorm analysis from 1993 to 2008. Journal of Geophysical Research. 116, A00I34, doi:10.1029/2010JA015788.

Wang H., H. Lühr, S. Y. Ma, P. Ritter (2005). Statistical study of the substorm onset: its dependence on solar wind parameters and solar illumination. Annales Geophysicae. 23, 2069-2079. doi:10.5194/angeo-23-2069-2005.

Yermolaev, Yu.I., Nikolaeva, N.S., Lodkina, I.G., Yermolaev, M.Yu.: (2009). Catalog of large-scale solar wind phenomena during 1976-2000. Cosmic Research (Engl. Transl.), 47, 81-94.